Electronic Supplementary Material (ESI) for Dalton Transactions.

F and rare V^{4+} doped cobalt hydroxide hybrid nanostructures: Excellent OER activity with ultralow overpotential

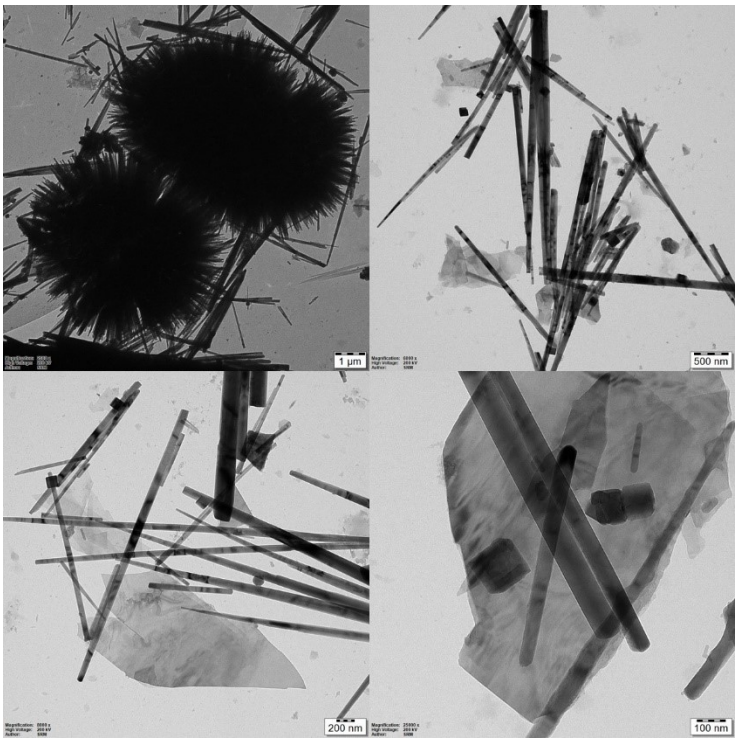

Figure S1. HR-TEM images of $Co(OH)_2$.

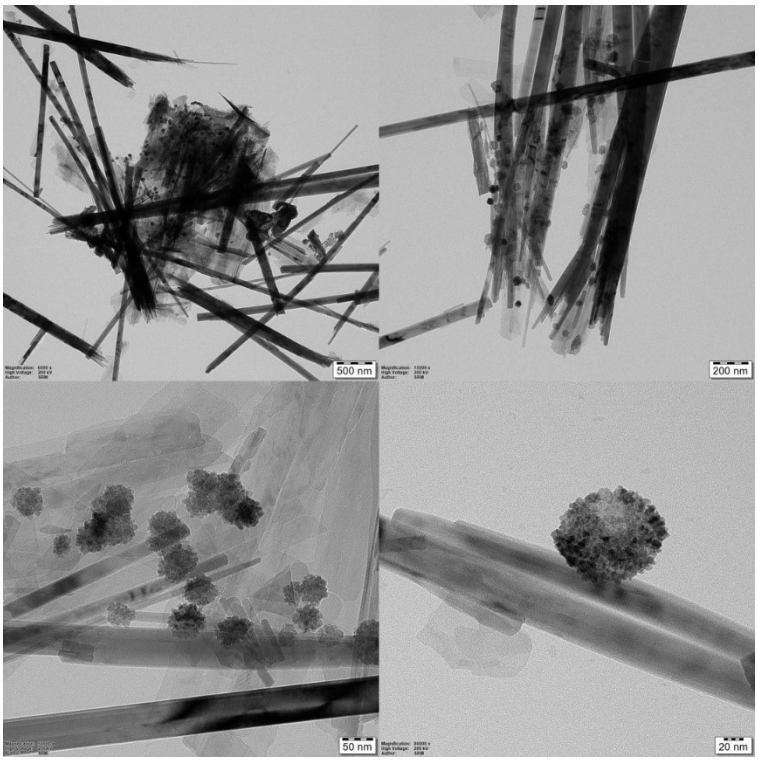

Figure S2. HR-TEM images of V-$Co(OH)_2$.

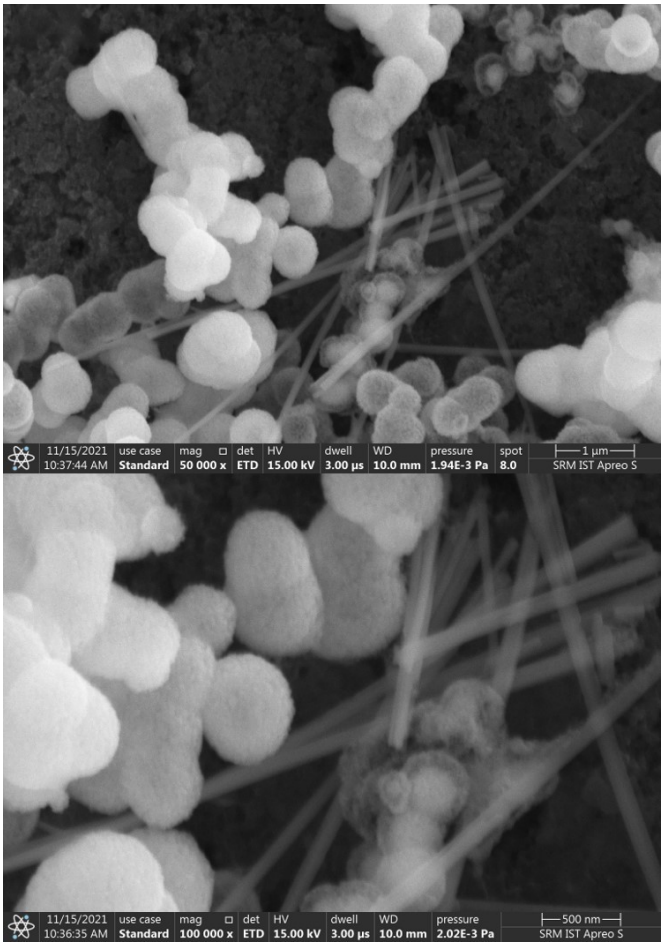

Figure S3. FE-SEM images of V-$Co(OH)_2$.

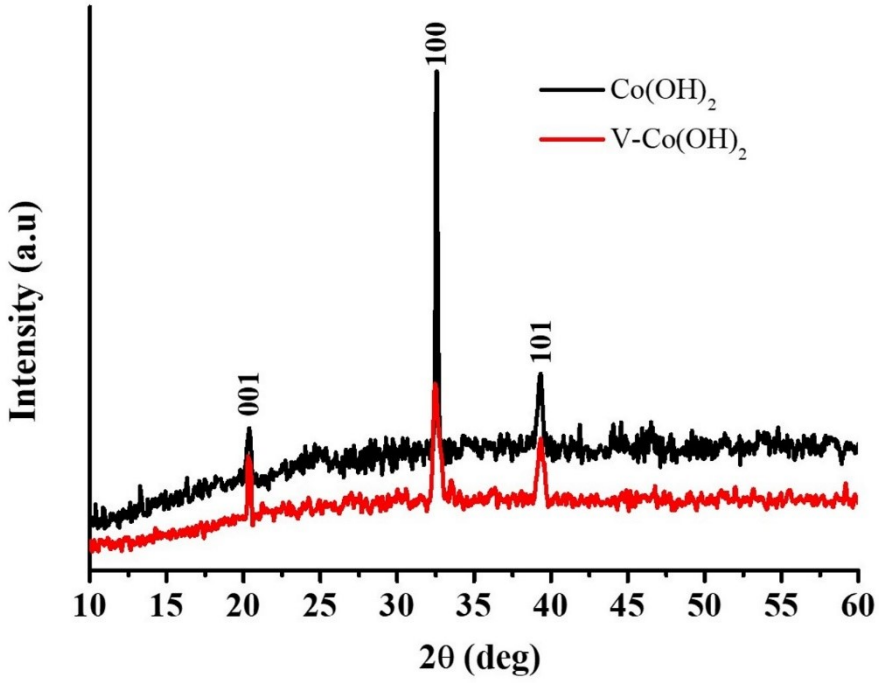

Figure S4. PXRD patterns of $Co(OH)_2$ and V-$Co(OH)_2$.

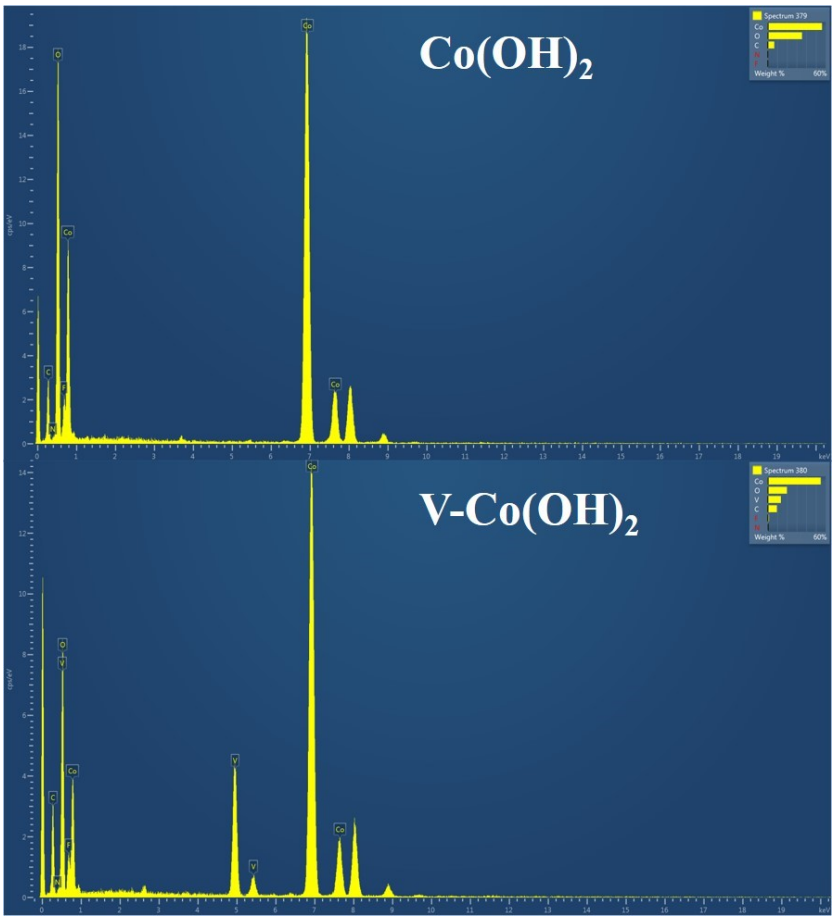

Figure S5. EDX graph of $Co(OH)_2$ and V-$Co(OH)_2$.

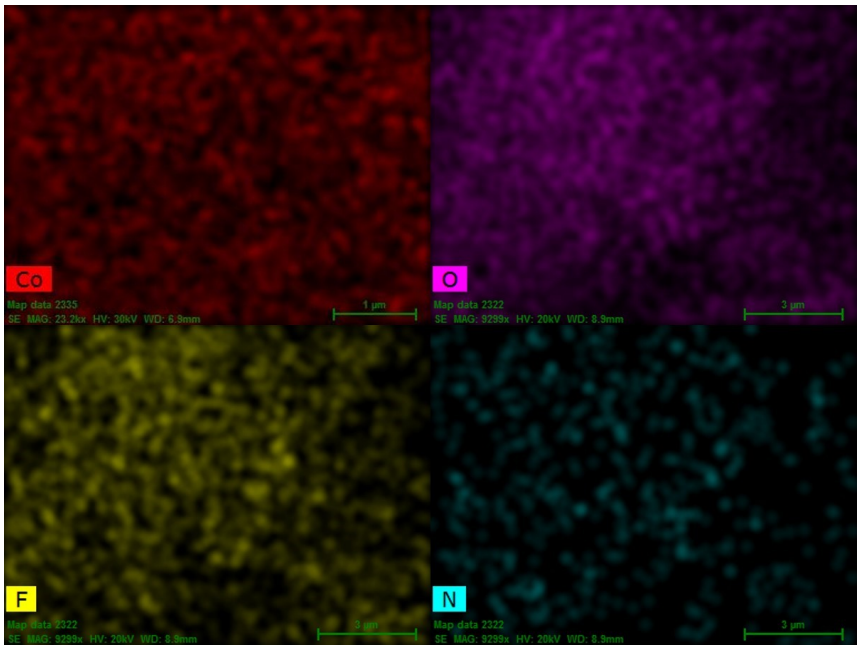

Figure S6. Elemental mapping of $Co(OH)_2$.

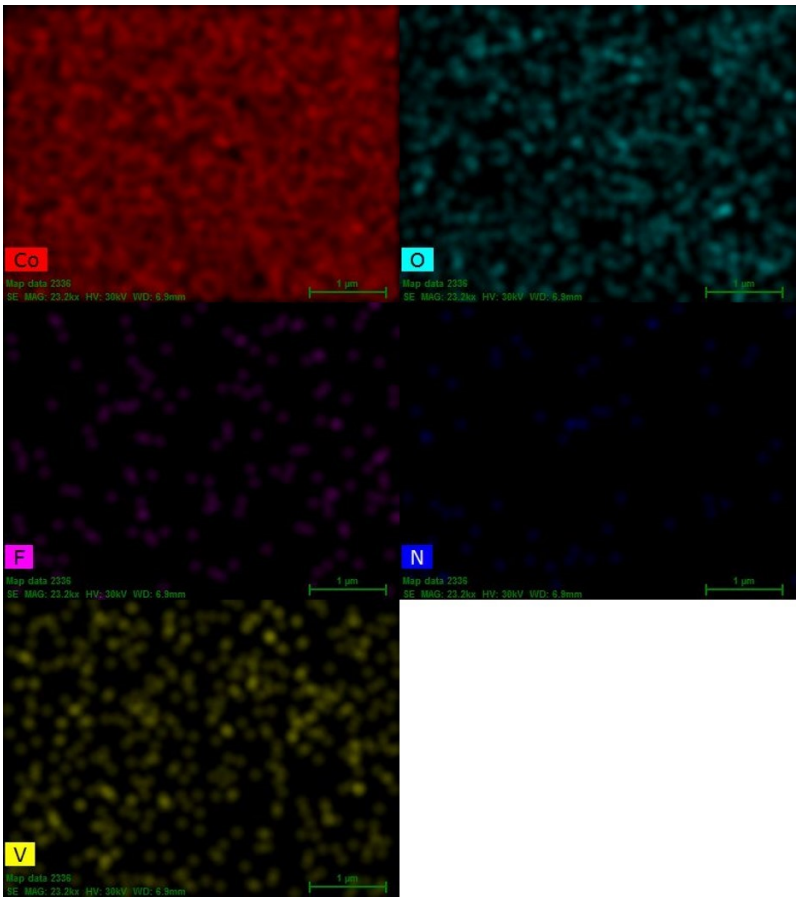

Figure S7. Elemental mapping of V-$Co(OH)_2$.

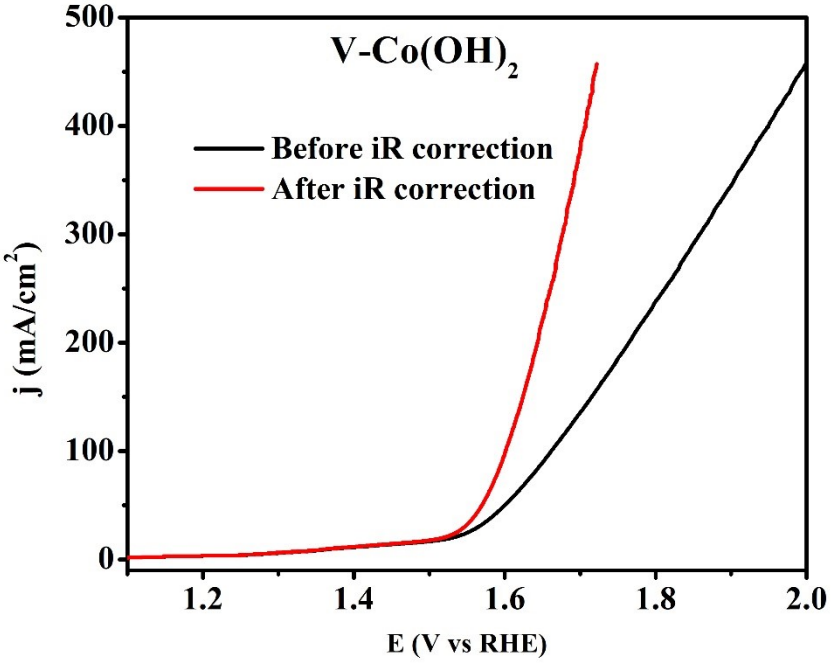

Figure S8. OER polarization curves of V-$Co(OH)_2$ before and after iR correction.

Table S1- Comparison table to comparing the OER activity of V-$Co(OH)_2$ with recently reported catalysts.

Catalyst	Overpotential at 10 mA cm^{-2} (mV)	Tafel Slope (mV/dec)	Reference
V-$Co(OH)_2$	**136**	**47.2**	**Our work**
V-doped CoP	254	35	1
V-Doped Co_3O_4	293.6	53.3	2
CoFeV LDH/NF	242	57	3
V-$Ni3S_2$/CC	180	56	4
CoVOOH	190	39.6	5
CoV-HNNs	268	80	6
CoFeV LDH	242	41.4	7
NiFeV LDHs	195 (20 j)	42	8
V-Co/CoO@C	320	143	9
V-Ni_3S_2	148	70	10
VO_x/Ni_3S_2@NF	358 (100 j)	82	11
V-doped CoP	340	95.7	12
Ru/CoFe LDH	198	39	13
V^{3+}-β-$Co(OH)_2$	198	60	14
CoVP@CC	290	55.9	15
V-NiFe-LDH/NF	195	31.3	16
V-Ni_3S_2@NiO/NF	170	98.8	17
Ni_1V_1P NSs/NF	250 (50 j)	80	18
Ru doped $Co(OH)_2$	305 (50 j)	64.8	19
Fe doped MOF CoV@CoO nanoflakes	220 (25j)	59	20
NiCoV-LDH	280	67	21
Co/VN	320	50.4	22

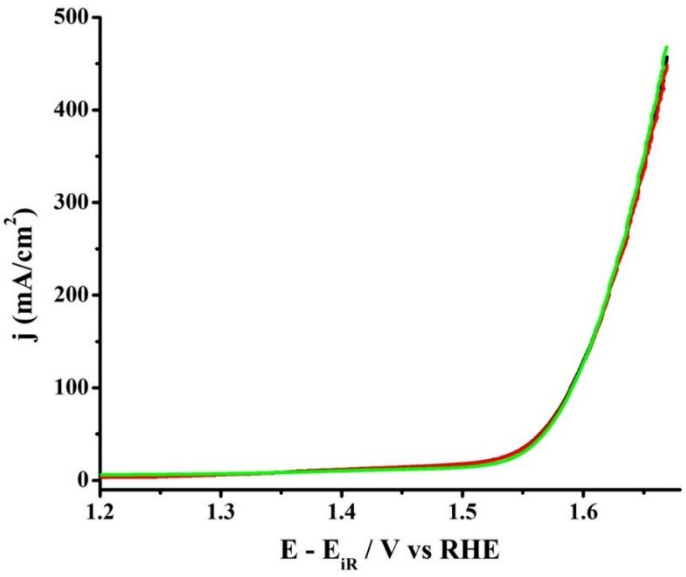

Figure S9. OER polarization curves of V-$Co(OH)_2$ fabricated at three different batches.

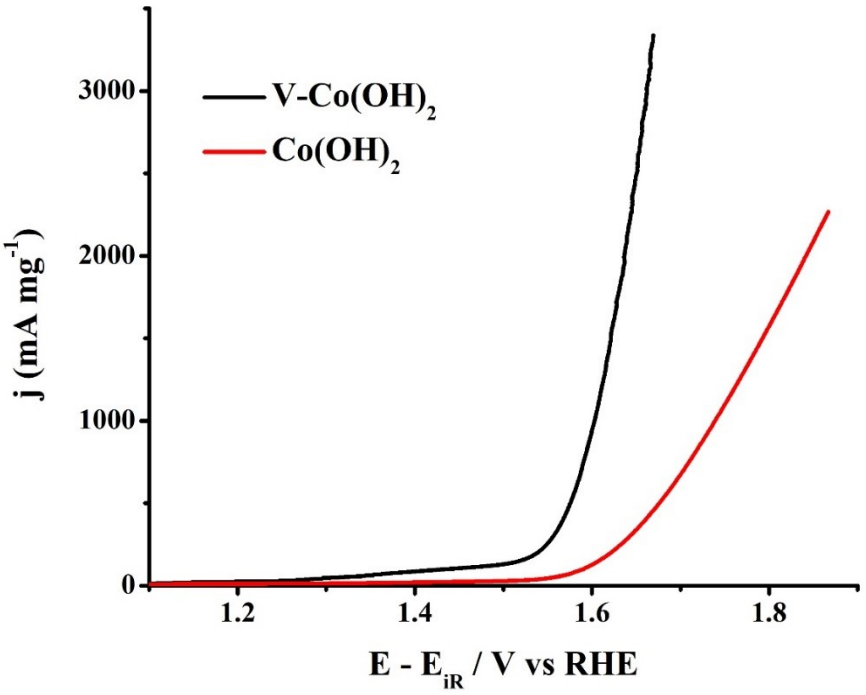

Figure S10. Mass activity of undoped $Co(OH)_2$ and V-$Co(OH)_2$ catalysts.

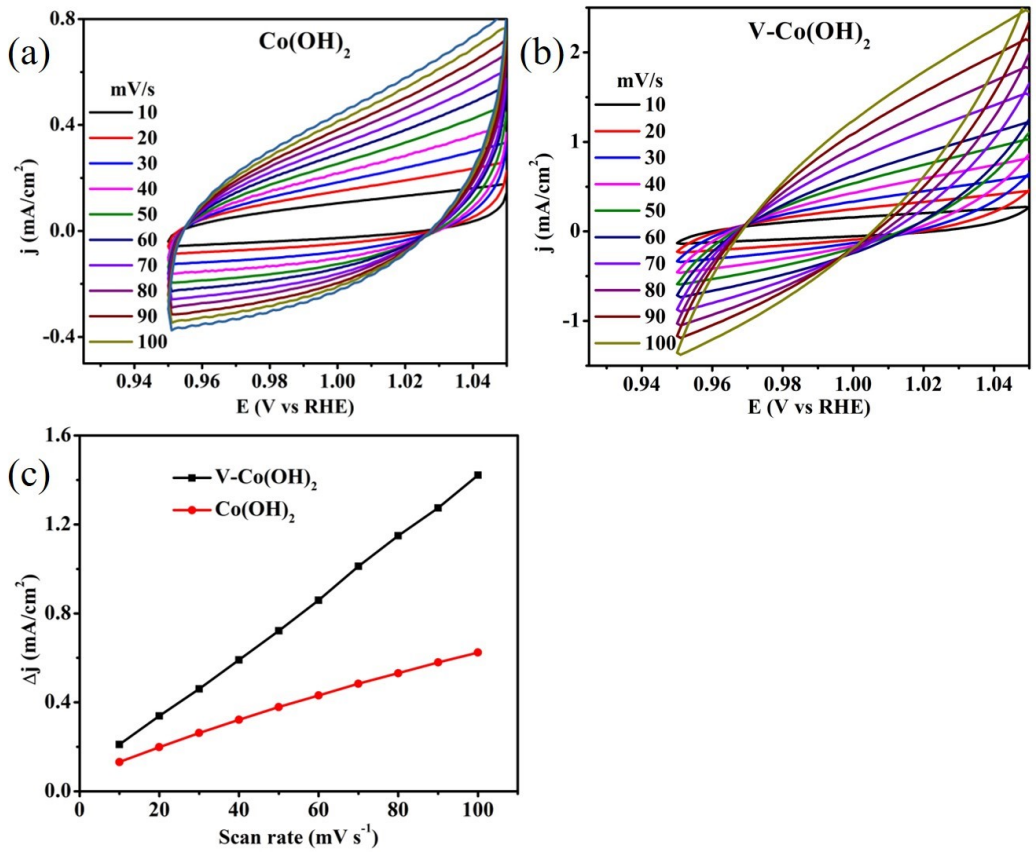

Figure S11. (a, b) Double layer capacitance and (c) capacitive currents as a functional of scan rate.

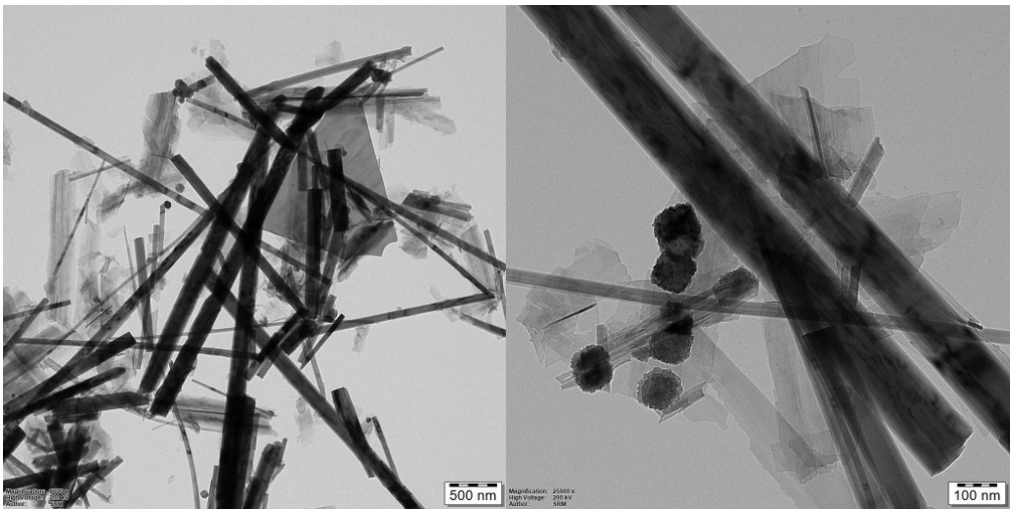

Figure S12. HR-TEM, SAED pattern and lattice fringe pattern images of V-$Co(OH)_2$-8.

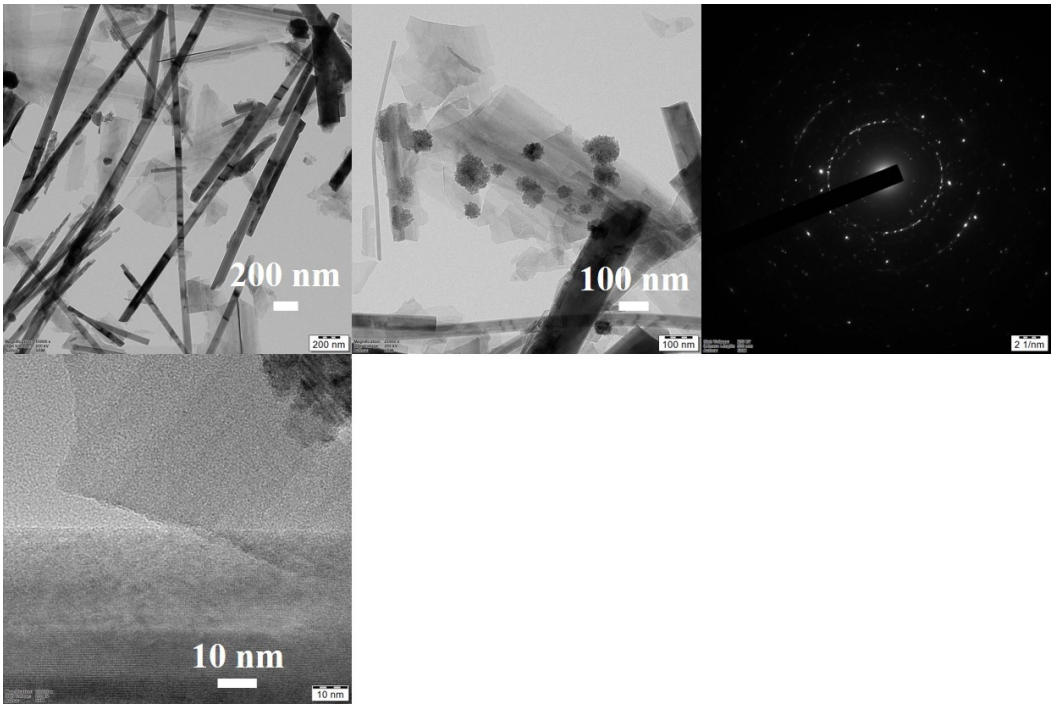

Figure S13. HR-TEM, SAED pattern and lattice fringe pattern images of V-$Co(OH)_2$-12.

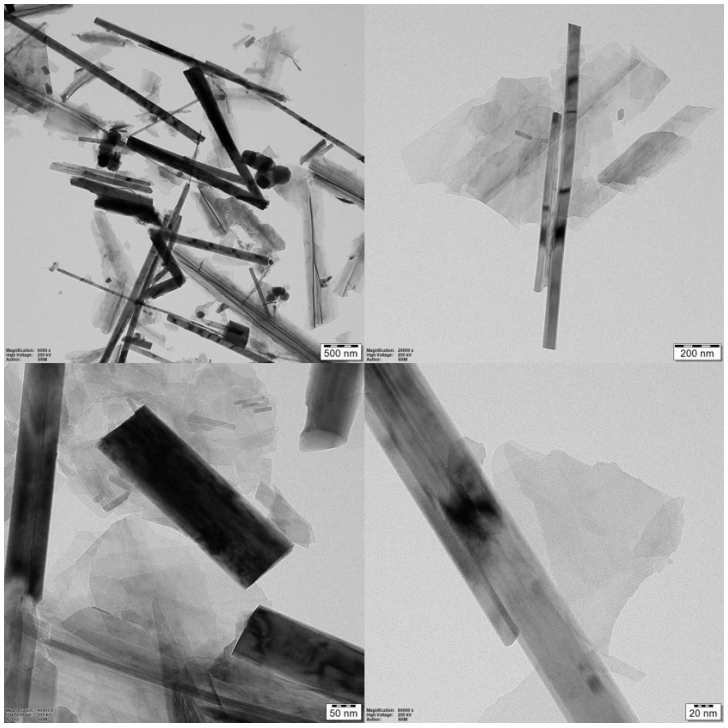

Figure S14. HR-TEM images of V-$Co(OH)_2$-12 at various magnification.

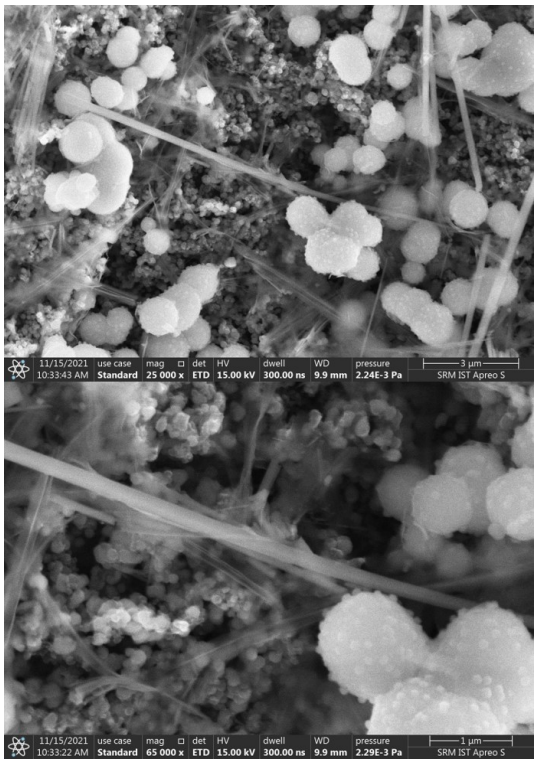

Figure S15. FE-SEM images of V-$Co(OH)_2$-8.

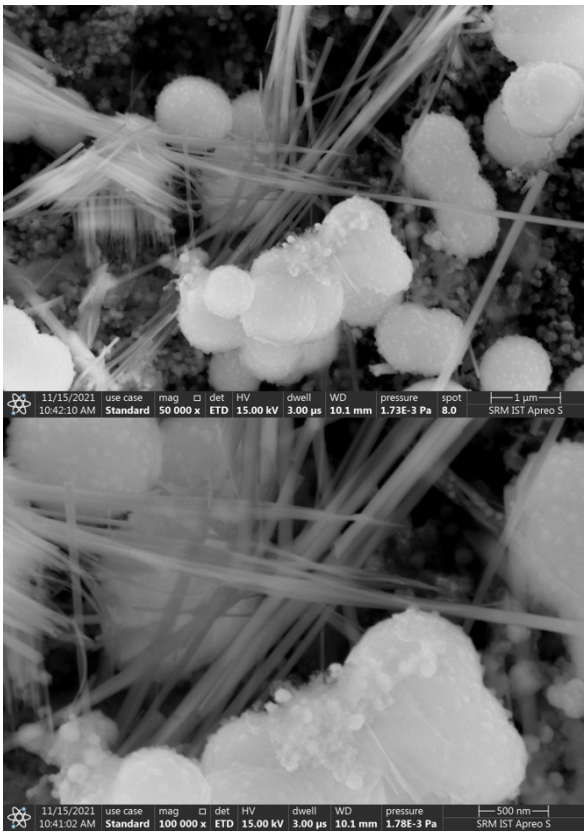

Figure S16. FE-SEM images of V-$Co(OH)_2$-12.

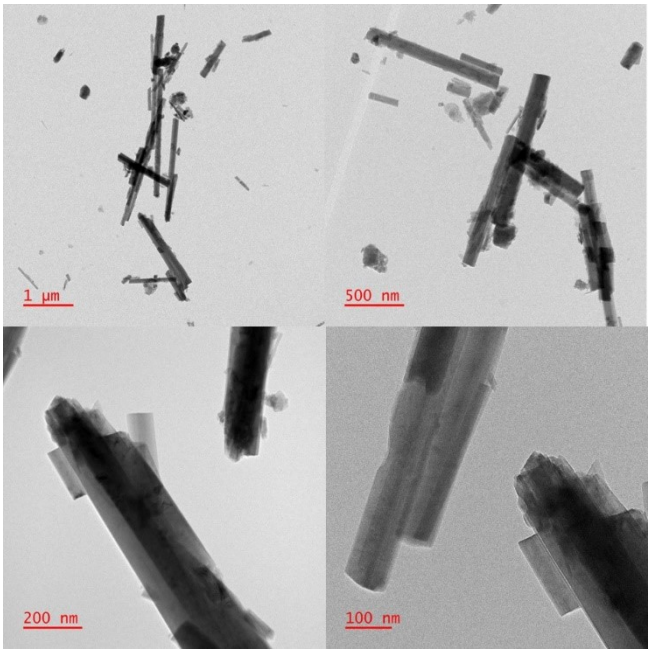

Figure S17. HR-TEM images of V-$Co(OH)_2$-2h.

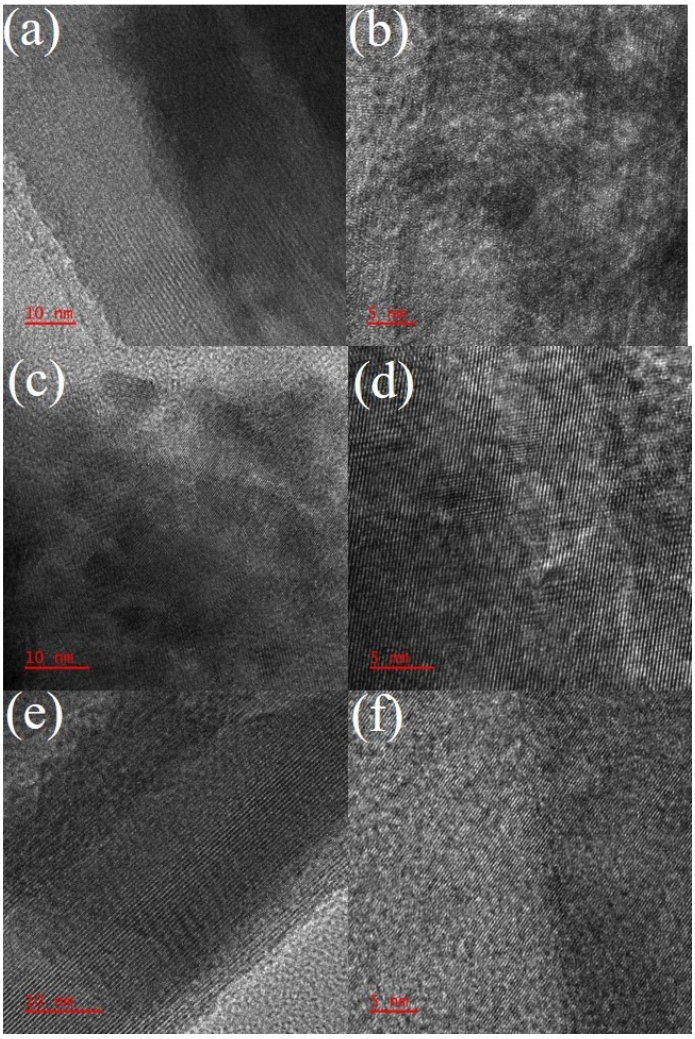

Figure 18. Lattice fringe pattern images of (a, b) V-$Co(OH)_2$-2h, (c, d) V-$Co(OH)_2$-4h and (e, f) V-$Co(OH)_2$ prepared without using NH_4F.

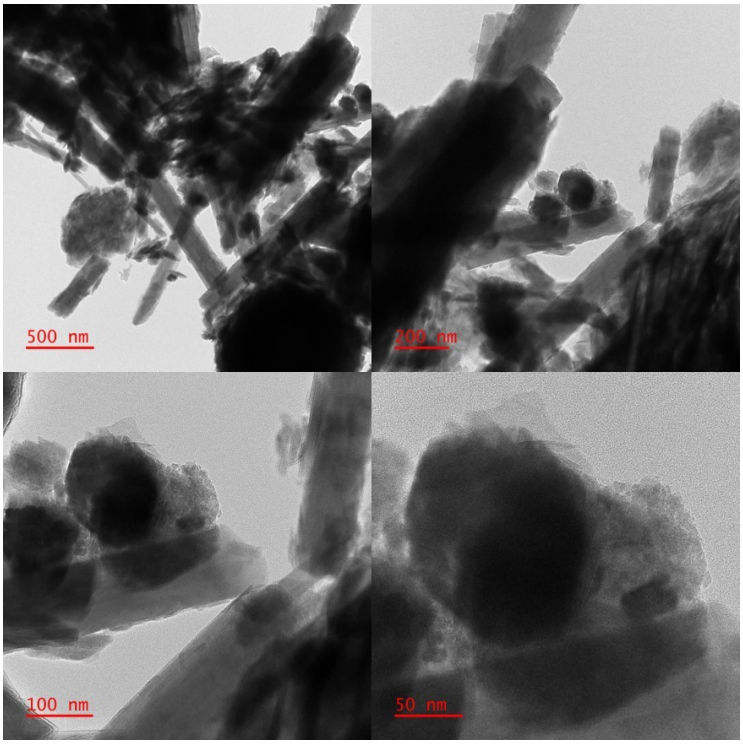

Figure S19. HR-TEM images of V-$Co(OH)_2$-4h.

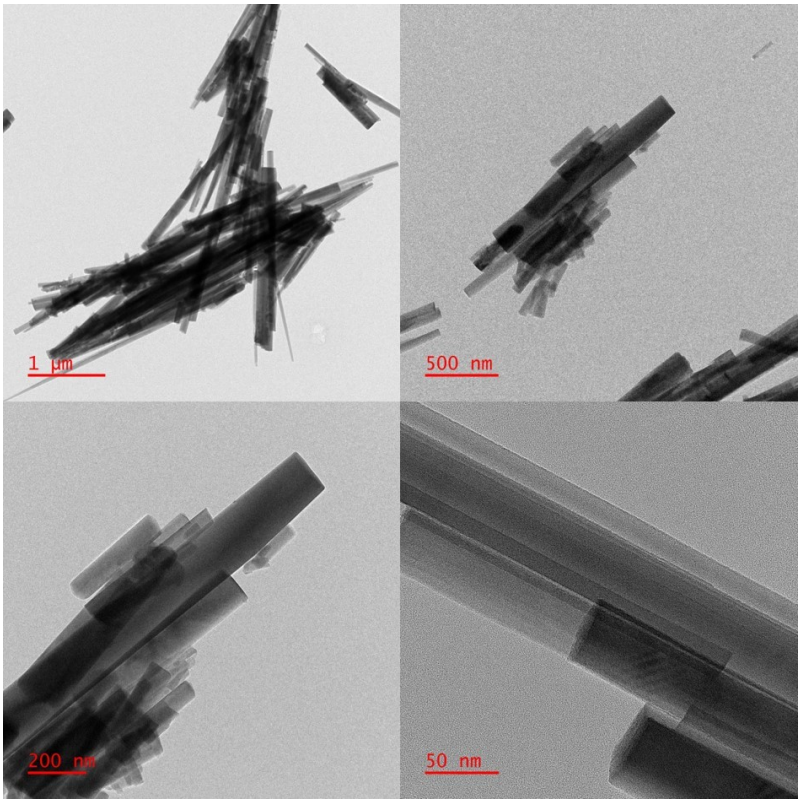

Figure S20. HR-TEM images of V-$Co(OH)_2$ without NH_4F.

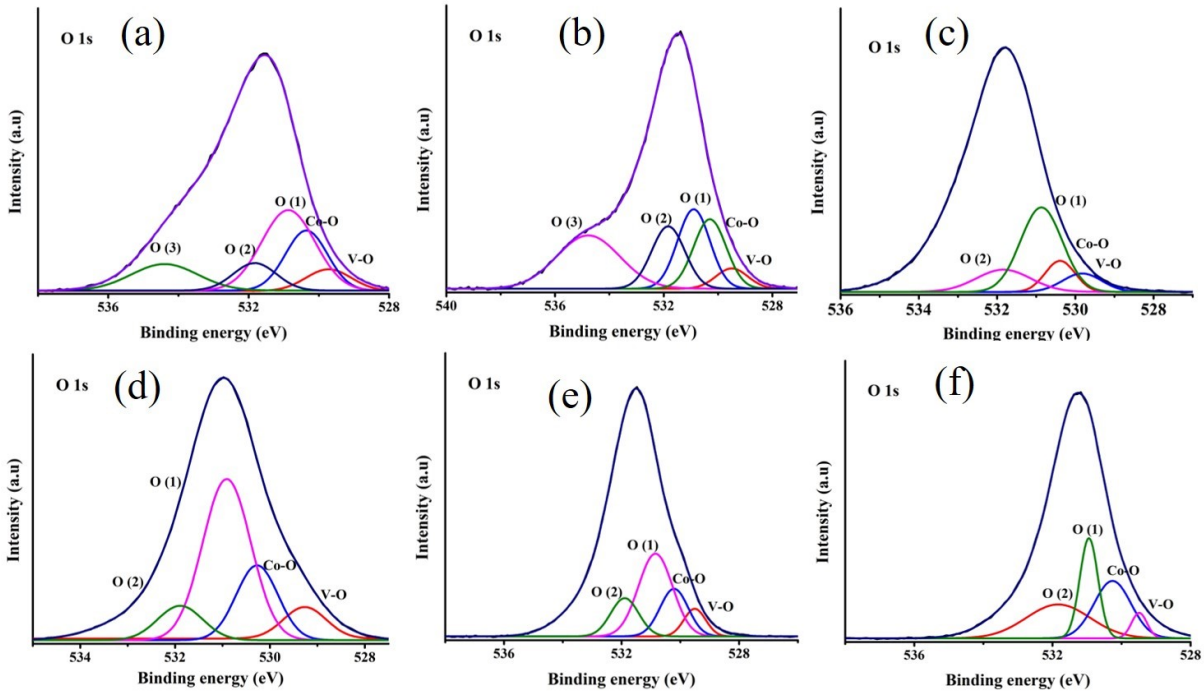

Figure S21. The high-resolution XPS spectra of O 1s in (a) V-$Co(OH)_2$-8, (b) V-$Co(OH)_2$-12, (c) V-$Co(OH)_2$-2h, (d) V-$Co(OH)_2$-4h, (e) V-$Co(OH)_2$ without NH4F and (f) V-$Co(OH)_2$ with NaF.

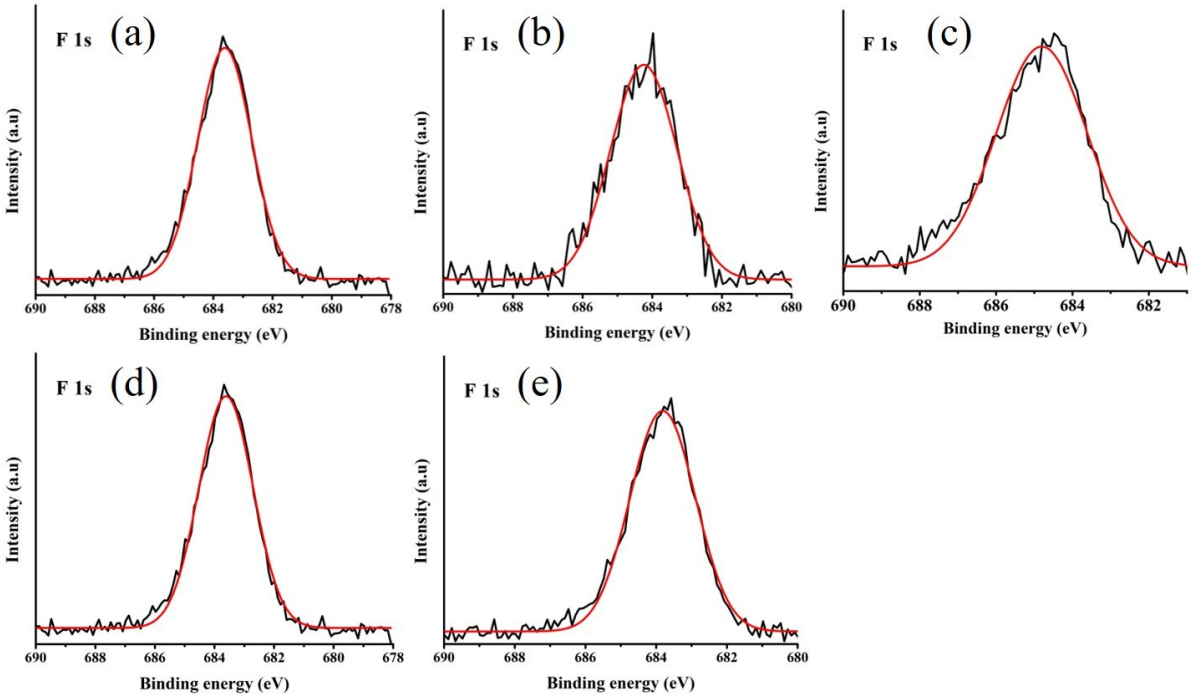

Figure S22. The high-resolution XPS spectra of F 1s in (a) V-$Co(OH)_2$-8, (b) V-$Co(OH)_2$-12, (c) V-$Co(OH)_2$-2h, (d) V-$Co(OH)_2$-4h, (e) with NaF.

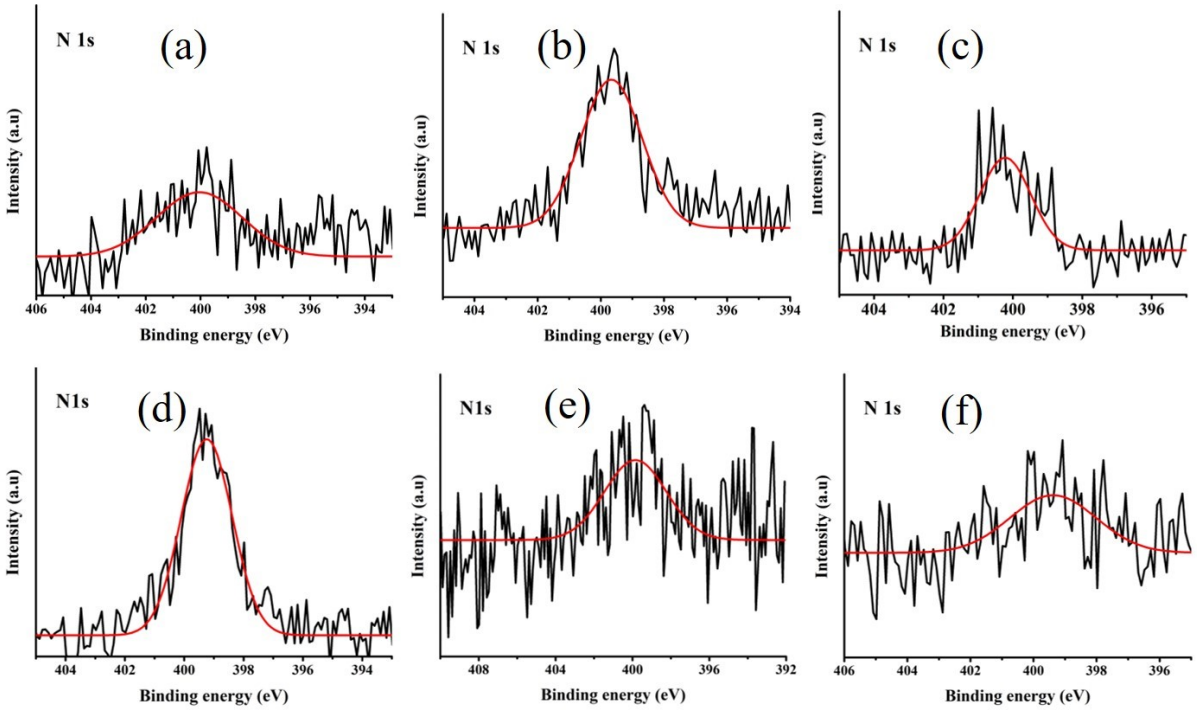

Figure S23. The high-resolution XPS spectra of N 1s in (a) V-$Co(OH)_2$-8, (b) V-$Co(OH)_2$-12, (c) V-$Co(OH)_2$-2h, (d) V-$Co(OH)_2$-4h, (e) V-$Co(OH)_2$ without NH_4F and (f) V-$Co(OH)_2$ with NaF.

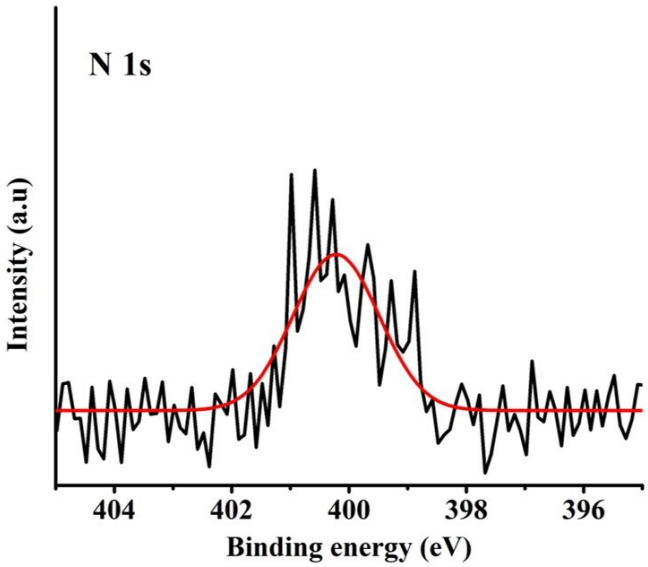

Figure S24. The high-resolution XPS spectra of N 1s in V-$Co(OH)_2$ after OER studies.

Table S2. Binding energy comparison of $Co(OH)_2$ and V, F doped catalysts.

Catalyst	**Binding energy (eV)**		**Intensity ratio (Co^{2+}/Co^{3+})**	**Binding energy (eV)**		**Intensity ratio (V^{4+}/V^{5+})**
	Co^{2+}	Co^{3+}		V^{4+}	V^{5+}	
$Co(OH)_2$	797.68	795.72	7.5>	-	-	-
	781.83	780.68	9.5>			
V-$Co(OH)_2$-8	798.15	795.72	3.2>	516.75	517.85	1.8>
	782.13	780.2	1.4>			
V-$Co(OH)_2$-10	798.01	795.71	2.0>	516.57	517.75	3.4>
	781.97	780.2	2.1>			
V-$Co(OH)_2$-12	798.3	796.5	2.9<	516.38	517.29	1.5>
	782.6	780.7	1.2<			
V-$Co(OH)_2$-2h	798.06	795.66	8>	516.12	517.87	5.0>
	782.32	780.15	4.9>			
V-$Co(OH)_2$-4h	798.04	796.3	2.4<	516.17	517.16	3.1>
	781.6	780.2	1.3<			
V-$Co(OH)_2$ (without NH_4F)	798.02	796.4	2<	516.62	517.94	3.0>
	781.71	779.86	1.3<			
V-$Co(OH)_2$-NaF	798.2	796.5	5.2<	516.17	517.15	2.0>
	781.72	780.2	1.2<			
V-$Co(OH)_2$-after OER	797.72	796.14	1.8<	516.5	517.36	1.3>
	781.67	780.37	1.3<			

References

[1] L. Liardet, X. Hu, *ACS Catal.* **2018**, *8*, 644–650.

[2] P. Li, X. Duan, Y. Kiang, Y. Li, G. Zhang, W. Liu, X. Sun, *Adv. Energy Mater.* **2018,** *8,* 1703341.

[3] Y. Hu, Z. Wang, W. Liu, M. Guan, Y. Huang, Y. Zhao, J. Bao, H.-M. Li, *ACS Sus. Chem. Eng.***2019,** 7, 16828-16834.

[4] L. Ma, K. Zhang, S. Wang, L. Gao, Y. Sun, Q. Liu, J. Guo, X. Zhang, *Appl. Surf. Sci.* **2019,** *489,* 815-823.

[5] Y. Cui, Y. Xue, R. Zhang, J. Zhang, X. Li, X. Zhu, ***J. Mater. Chem. A*** **2019**, *7*, 21911-21917.

[6] M. Yang, X. Fu, M. Shao, Z. Wang, L. Cao, S. Gu, M. Li, H. Cheng, Y. Li, H. Pan, Z. Lu, *ChemElectroChem,* **2019,** *6,* 2050-2055.

[7] Y. Yang, Y. Ou, Y. Yang, X. Wei, D. Gao, L. Yang, Y. Xiong, H. Dong, P. Xiao, Y. Zhang, ***Nanoscale*** **2019**, ***11***, 23296-23303.

[8] R. Wei, X. Bu, W. Gao, R. A. B. Villaos, G. Macam, Z.-Q. Huang, C. Lan, F.-C. Chuang, Y. Qu, J. C. Ho, *ACS Appl. Mater. Interfaces* **2019**, *11*, 33012–33021.

[9] H. Huang, Y. Li, W. Li, S. Chen, C. Wang, M. Cui, T. Ma, *Inorg. Chem. Commun.* **2019,** *103,* 1-5.

[10] J. Guo, K. Zhang, Y. Sun, Q. Liu, L. Tang, X. Zhang, ***Inorg. Chem. Front.***, 2019,**6**, 443-450.

[11] Y. Niu, W. Li, X. Wu, B. Feng, Y. Yu, W. Hu, C. M. Li, ***J. Mater. Chem. A*** **2019**, *7*, 10534-10542.

[12] J.-F. Qin, J.-H. Lin, T.-S. Chen, D.-P. Liu, J.-Y. Xie, B.-Y. Guo, L. Wang, Y.-M. Chai, B. Dong, *J. Energy Chem.* **2019,** *39,* 182-187.

[13] P. Li, M. Wang, X. Duan, L. Zheng, X. Cheng, Y. Zhang, Y. Kuang, Y. Li, Q. Ma, Z. Feng, W. Lu, X. Sun, *Nat. Commun.* **2019,** *10,* 1711.

[14] S. Anantharaj, K. Karthick, P. Murugan, S. Kundu, *Inorg. Chem.* **2020**, *59,* 730-740.

[15] H. Han, F. Yi, S. Choi, J. Kim, J. Kwon, K. Park, T. Song, *J. All. Comp.* **2020,** *846,* 156350.

[16] J. Liang, H. Shen, Y. Ma, D. Liu, M. Li, J. Kong, Y. Tang, S. Ding, ***Dalton Trans.*** **2020**, ***49***, 11217-11225.

[17] Q. Liu, J. Huang, L. Cao, K. Kajiyoshi, K. Li, Y. Feng, C. Fu, L. Kou, L. Feng, *ACS Sustainable Chem. Eng.* **2020**, *8*, 6222–6233.

[18] Y. Li, X. Jiang, Z. Miao, J. Tang, Q. Zheng, F. Xie, D. Lin, *ChemcatChem,* **2020,** *12,* 917-925.

[19] Y. Zhu, D. Cao, N. Liu, D. Cheng, *Int. J. Hyd. Energy* **2021,** *46,* 22832-22841.

[20] A. Mutharasu, A. P. Tiwari, K. Chhetri, B. Dahal, H. K. Kim, *Nano Energy* **2021,** *88,* 106238.

[21] K. Bera, A. Karmakar, S. Kumaravel, S. S. Sankar, R. Madhu, H. N. Dhandapani, S. Nagappan, S. Kundu, *Inorg. Chem.* **2022**, *61*, 4502–4512.

[22] X. Peng, C. Huang, J. Dai, Y. Liu, *Int. J. Hyd. Energy* **2022,** *47,* 4386-4393.